



Comparison of CO₂ gasification reactivity and kinetics: petcoke, biomass and high ash coal

Neelam Kumari¹ · Sujan Saha¹ · Gajanan Sahu¹ · Vishal Chauhan¹ · Rupak Roy¹ · Sudipta Datta¹ · Prakash D. Chavan¹

Received: 4 May 2020 / Revised: 3 July 2020 / Accepted: 8 July 2020 / Published online: 22 July 2020
© Springer-Verlag GmbH Germany, part of Springer Nature 2020

Abstract

It is desirable to exploit biomass energy along with coal and petcoke through gasification, and understanding the differences between petroleum coke (petcoke), coal and biomass gasification behaviour becomes very essential. Consequently, present investigation compares gasification components of petcoke, sawdust and high ash coal with their physico-chemical properties under isothermal conditions in CO₂ atmosphere in the temperature range of 1173–1623 K. Physico-chemical characterisation includes proximate and ultimate analyses, porous structure analysis by Brunauer-Emmett-Teller (BET) surface area from nitrogen (N₂) adsorption isotherm, ash composition analysis and ash fusion temperature. The effects of temperature and nature of different solid fuels on gasification reactivity have been discussed. Gasification kinetics has been investigated using two *n*th-order kinetic models, such as homogeneous model (HM) and shrinking core model (SCM). Influence of diffusion resistance on gasification behaviour of different solid fuels is also reported. Thus, the present study will be helpful to realise the effects of high ash in gasification behaviour as well as in designing and modelling of the suitable gasifier and to establish optimum gasification conditions for petcoke, biomass and high ash coal.

Keywords Gasification · Reactivity · Kinetics · High ash coal · Sawdust · Petcoke

1 Introduction

Petroleum coke or petcock is a carbonaceous material consisting of polycyclic aromatic hydrocarbon. It is a by-product of crude oil processing by thermal cracking followed by delayed or fluid coking. Petcoke production in refineries is gradually climaxing due to the increasing trend of heavy crude processing as well as the maximising economic benefit from every single refinery stream. Presently, world production of petcoke is around 150 million metric ton per annum (MMTPA) and in India, it is about 15 MMTPA [1]. High calorific value, low ash, abundant availability and relatively cheaper price of petcoke make it an attractive energy resource and worldwide utilisation of petcoke is dominated in the energy sector (75%) as fuel or process feedstock. Non-energy

usages of petcoke basically include the production of carbon anodes for aluminium industry and graphite electrodes for steel industry [2].

Traditionally, petcoke is burned in a boiler for power or heat generation. Nevertheless, high sulphur and vanadium content of petcoke imposes serious environmental and operational issues. Considering severe air pollution, the apex court of India banned the use of petcoke in Delhi and the National Capital Region (NCR) area since 1 November 2017 [3] and further imposed ban on import of petcoke in India for its use as fuel since 26 July 2018 [4]. China has also reduced the import of petcoke significantly from 2014. In this context, gasification of petcoke which is legally allowed by the apex court of India [4] may be an effective option towards its judicious utilisation to produce power, heat and various chemicals, such as ammonia, urea, methanol and F-T liquids meeting stringent environmental regulations.

On the other hand, India has a vast reserve of coal and generates a significant amount of biomass residue. Presently, India is the 2nd coal producer country in the world with its estimated non-coking coal reserve of 170.68 BT up to the depth of 300 m. Furthermore, out of this vast reserve, inferior grade high ash non-coking coal (grade G7 to grade G17)

✉ Sujan Saha
sjan_1976@yahoo.co.in; sujansaha@cimfr.nic.in

¹ Gasification, Catalysis and CTL Research Group, CSIR-Central Institute of Mining & Fuel Research (CIMFR), P.O. FRI, Digwadih Campus, Dhanbad, Jharkhand 828108, India

mostly dominates with its share of 82.5% [5]. Being an agricultural nation, biomass availability in India is more than 500 MMT/year, and this large biomass energy utilisation is very crucial in India's future energy planning [6]. Biomass energy is always attractive and effective option to reduce carbon emissions to the environment as it is renewable and carbon neutral. Moreover, use of biomass as gasification or combustion feedstock is always advantageous owing to its higher reactivity resulting from high volatile content, inorganic constituents and structural make-up. However, industrial utilisation of biomass is considerably constrained due to its lower energy content, lower bulk density, higher tar yield and most unstable supply chain resulting from its spatiotemporal nature [7]. Therefore, it might be desirable to exploit biomass energy along with coal and petcoke through gasification, and understanding the differences of petcoke, coal and biomass gasification behaviour becomes very essential.

In this context, several researchers worked in the area of CO₂-char gasification kinetics of different carbonaceous materials. CO₂-char reaction is important as it is the slowest among gasification reactions and considered as the rate-determining step as well as to make a balance between air or oxygen and steam to generate optimum heat for driving endothermic gasification reactions [8, 9]. Therefore, sound knowledge of CO₂-char gasification reactivity and kinetics is essential to establish process parameters and to design and develop suitable gasifiers for different energy resources, such as coal, biomass and petcoke. Heterogeneous char gasification reaction is a complex phenomenon controlled by various factors, such as physico-chemical properties and reaction conditions [8–13]. Isothermal CO₂ gasification kinetics of petcoke, coal and biomass in the temperature range of 1123–1573 K using a thermogravimetric analyser (TGA) was studied by Huo et al. [9]. They explained the influence of the physical characteristics of different feed materials on gasification activities. Ding et al. [14] explored rapid pyrolysis and in situ gasification characteristics of coal and petcoke using a microscope coupled to a TGA. Furthermore, a comparison of steam gasification characteristics of coal char with petcoke-char in the temperature range of 1373–1673 K in a drop tube furnace was studied by Ding et al. [15]. They described the effects of steam concentration, gasification temperature and types of carbonaceous material on gasification characteristics. Petcoke and lignite gasification under CO₂ atmosphere using the isothermal thermogravimetric method at 1273 K was studied by Zhan et al. [16]. They reported very poor reactivity of petcoke which was improved by blending with lignite. Isothermal CO₂ gasification reactivity of different carbonaceous materials including petcoke and coal in the temperature ranging from 1223 to 1673 K by the thermogravimetric method was reported in the literature [17]. It was found that the petcoke reactivity was several times poorer than coal chars. Apparent activation energies of different feed materials were also

mentioned. Feroso et al. [18] studied gasification reactivity and kinetics of coal, biomass and petcoke using the isothermal thermogravimetric method in the temperature range of 1123–1323 K. They reported higher reactivity of biomass than coal and petcoke due to the catalytic effects of biomass ash.

Furthermore, isothermal gasification kinetics of 13 carbonaceous materials including coal of different ranks and petcoke in CO₂/steam in the temperature range of 1273–1873 K using a drop-in-fixed-bed reactor under atmospheric pressure was explored by Ren et al. [19]. The experimental results reflected that the increasing gasification temperature levelled off the difference in gasification reactivity among the samples. However, gasification reactivity of petcoke even at 1873 K was too low to compete with coal and it was 2–9 times slower than that of coal. Physical properties and CO₂ gasification reactivity of petcoke and coal char in the temperature range of 1223–1673 K were also investigated by Wu et al. [20]. They showed the effects of pyrolysis temperature and pyrolysis pressure on gasification activity. Results revealed that the effects of temperature and pressure of pyrolysis were significantly different for coal and petcoke.

Therefore, a detailed literature survey reflects that though many researchers have worked in the area of gasification behaviour of petcoke, coal and biomass, there is a scarcity of literature to compare gasification behaviour of high ash coal (>40%), petcoke and biomass. Consequently, the aim of the present investigation is to compare gasification components of petcoke, biomass and high ash coal with their physico-chemical properties under isothermal conditions in CO₂ atmosphere in the temperature range of 1173–1623 K. Physico-chemical characterisation includes proximate and ultimate analyses, porous structure analysis by Brunauer-Emmett-Teller (BET) surface area from nitrogen (N₂) adsorption isotherm, ash composition analysis and ash fusion temperature. Variation of gasification reactivity with temperature and nature of different chars has been discussed. Gasification kinetics is investigated using two *n*th-order kinetic models, such as homogeneous model (HM) and shrinking core model (SCM). Influence of diffusion resistance on gasification behaviour of different solid fuels is also reported. Thus, the present study will be helpful to realise the effects of high ash in gasification behaviour as well as in designing and modelling suitable gasifier and to establish optimum gasification conditions for petcoke, biomass and high ash coal.

2 Experimental

2.1 Selection of carbonaceous solid fuels

The carbonaceous solid fuels used in this investigation incorporated one high ash coal (HAC, ash content 41.3%), one petcoke (PC) and one sawdust (SD) samples. HAC was

collected from one Indian coal field, while PC and SD were taken from Indian refinery and local timber industry, respectively. For feed material characterisation and gasification experiments, all the samples were crushed to the particle sizes range of $-0.21 + 0.15$ mm. Proximate and ultimate analyses of all the feed materials have been depicted in Table 1. Proximate and ultimate analyses of PC, SD and HAC were conducted following ASTM standards and Indian standards [7, 8, 21–24]. Table 1 clearly indicates that these carbonaceous substances differ significantly in ash, volatile matter and fixed carbon as well as in their elemental constituents.

2.2 Char preparation

Gasification of any carbonaceous material occurs in two steps. The first step is the pyrolysis which produces char and volatiles. The second step is the char gasification step to convert solid char to gaseous products. This is the slowest step and, hence, rate-determining step. In the gasifier, coal particles are first dried by the hot gases (product gas comprising of mainly CO and H₂) and pyrolysis starts as the temperature of the coal particle exceeds 673 K and continues up to higher temperature ~1273 K. Liquids, such as tars, oils and phenols, and hydrogen-rich volatile hydrocarbon gases are formed. The residue as char contains the remaining carbon and mineral matter. After attaining a temperature of 973 K or more, char gasification reactions begin [25]. Therefore, to study pure char gasification reaction separating from devolatilisation, char samples from petcoke, sawdust and coal were prepared keeping in mind the facts of complete removal of volatiles as well as avoiding rearrangement of the material surface [26].

For the present investigation, char samples were prepared at 1173 K in nitrogen (N₂) atmosphere (purity 99.999%) by STA 449 F3 Jupiter TGA (Netzsch, Germany). A flat alumina sample container was used to hold about 500 mg of sample. Then, the temperature was increased up to 1173 K at the ramp rate of 10 K/min in N₂ flow of 100 ml/min and the sample kept for 30 min more at that temperature to eliminate volatiles completely. Similar experiments were conducted to have an

adequate amount of char for performing different char characterisation and gasification experiments.

2.3 N₂ adsorption study

N₂ adsorption analysis was conducted to determine BET surface area by means of Brunauer-Emmett-Teller (BET) equation assuming multi-molecular layer adsorption of adsorbate gas on a solid adsorbent. Tristar 3000 of Micromeritics, USA, was used to measure BET surface area at liquid N₂ boiling temperature, i.e. 77 K using 99.999% pure N₂ as adsorbate gas in the relative pressure range of 0.05 to 0.3. For all the experiments, straight lines with correlation coefficients of greater than 0.99 were obtained and surface area was computed by the instrument software utilising the values of slope and intercept of the straight line [8, 26, 27]. BET surface area of raw and char samples of different carbonaceous substances are shown in Table 2. It may be noted that the surface of each sample was cleaned before conducting experiments by purging N₂ gas for 3 h at 423 K in a separate unit (FlowPrep of Micromeritics, USA).

2.4 Ash composition analysis

Petcoke ash, sawdust ash and coal ash were prepared following ASTM and Indian standard methods [8, 22, 28, 29]. Ash composition analysis was performed by using a wavelength-dispersive x-ray fluorescence (WDXRF) spectrometer (PW 2424 MagiX, Philips, The Netherlands) [8, 13, 22, 26]. Sample preparation is substantial during quantitative measurement by XRF specifically for solid powdered samples, where particle size, surface roughness and packing density affect analyte line intensity. Ash particle size of less than 200 mesh (BIS size) was achieved by an automatic grinder (Mini Mill, Fritsch). Stearic acid was used as a binder in pellet preparation with sample and binder ratio of 10:1. Subsequently, the sample was pressed for 5 min under 150 kN forces using a Herzog TP 20 P hydraulic press and a stable pellet of 40 mm diameter was produced. Precise and accurate ash composition analysis of petcoke, biomass and coal has been depicted in Table 3.

Table 1 Proximate and ultimate analysis^b

Solid fuel ^a	Proximate analysis (wt.%, air-dried basis)				Ultimate analysis (wt.%, dry ash free basis)				
	M	A	VM	FC	C	H	N	S	O
PC	0.9	0.7	11.4	87.0	87.85	3.56	1.54	5.26	1.79
SD	10.8	3.7	65.7	19.8	49.72	6.20	0.36	-	43.72
HAC	6.5	41.3	24.5	27.7	71.17	5.42	1.65	1.05	20.71

^a PC, SD and HAC stand for petcoke, sawdust and high ash coal, respectively

^b Proximate analysis (wt.%, air-dried basis), ultimate analysis (wt.%, dry ash free basis). *M* moisture, *A* ash, *VM* volatile matter, *FC* fixed carbon, *C* carbon, *H* hydrogen, *N* nitrogen, *S* sulphur, *O* oxygen

Table 2 BET surface area of carbonaceous substances

Sample	BET surface area (m ² /g)	Sample	BET surface area (m ² /g)
PC	0.89	PC char	17.07
SD	0.46	SD char	593.26
HAC	16.92	HAC char	24.67

2.5 Determination of ash fusion temperature

Four important ash fusion temperatures (AFT), namely initial deformation temperature (IDT), softening temperature (ST), hemispherical temperature (HT) and flow temperature (FT), were measured using a heating microscope (5E-AF-4000, CKIC, China) in reducing conditions (IS-12891-1990). Ash sample (particle size -0.21 mm) was placed on a small platinum plate and was introduced into the furnace. As the temperature increased, the microscope projected image of the specimen and above-mentioned four temperatures of the ash samples were measured. During the experiment, the temperature was raised up to 1273 K at the rate of 10 K/min and then the heating rate was maintained 5 K/min up to 1773 K in order to obtain very accurate and precise measurements of ash fusion temperatures. Four important ash fusion temperatures of the samples have been depicted in Table 4.

2.6 Isothermal CO₂ gasification experiments by thermogravimetric method

The thermogravimetric analyser (TGA) is extensively accepted for gasification reactivity and kinetic analysis owing to its precise and accurate measurements as well as simple operation [29]. Isothermal gasification experiments in the present investigation were performed by using an STA 449 F3 Jupiter TGA (Netzsch, Germany) in the temperature range of 1173–1623 K in CO₂ atmosphere (purity 99.999%). The said TGA was capable to measure weight changes with a high resolution of 1 µg and low drift in microgram range over several hours along with accurate temperature determination having deviation up to 1.5 °C or 0.25%, whichever is greater. About 20 mg of char sample (particle size, $-0.21 + 0.15$ mm) was placed uniformly on a flat alumina container of the TGA for each experiment. First, it was heated up to the desired temperature in N₂ atmosphere (purity 99.999%) at the ramp rate of 10 K/

min. Post realisation of the target temperature, N₂ flow (100 ml/min) was replaced by CO₂ (purity 99.999%) of the same flow rate to conduct a gasification experiment at that desired temperature for 120 min. The TGA was calibrated and a blank run was conducted to negate the buoyancy effect associated with each experiment. The repeatability and accurateness of the TGA were confirmed by carrying out experiments with a reference sample (calcium oxalate).

3 Results and discussion

3.1 BET surface area of different carbonaceous substances and char

BET surface areas of PC, SD, HAC and their char samples prepared at 1173 K have been shown in Table 2. It clearly demonstrates that char samples have a higher surface area than the corresponding raw substances. It may be attributed to the creation of new pores due to the release of volatiles from carbon framework, opening up of previously closed pores as well as enlargement of already open pores with the heat treatment [8, 30]. An increase in surface area is highest in the case of SD char due to its higher volatile content. It may be mentioned that biomass, petcoke and coal are basically composed of polycyclic aromatic hydrocarbon building blocks connected by cross-links with heteroatom functional groups at their periphery. Pore structure is largely dependent on these cross-links and functional groups. The higher amount of cross-links and oxygen functional groups in biomass and coal leads to the larger volatiles which on removal during heating produce more porous chars. On the other hand, the structural make-up of petcoke with less volatiles and less oxygen functional groups makes it less porous. This observation is in accordance with the other researchers also [9, 31–33].

3.2 Ash characteristics

The chemical composition of ash is very important towards the selection of feed material for a particular gasifier. Ash fusion temperature (AFT) and slag flow depend on the chemical composition of ash. For an entrained flow gasifier, the operating temperature must be above AFT to maintain the slag in the Newtonian flow region. Continuous slag tapping is very

Table 3 Ash composition analysis and alkali index

Sample	Fe ₂ O ₃ (%)	CaO (%)	MgO (%)	Na ₂ O (%)	K ₂ O (%)	SiO ₂ (%)	Al ₂ O ₃ (%)	TiO ₂ (%)	P ₂ O ₅ (%)	SO ₃ (%)	V ₂ O ₅ (%)	NiO (%)	Alkali Index (AI)
Petcoke	6.39	15.12	1.35	1.37	0.82	21.27	9.76	0.75	0.67	1.23	31.23	10.04	0.57
SD	3.52	42.97	6.23	2.96	12.03	21.95	6.31	0.33	3.65	----	----	----	8.87
HAC	5.59	1.85	0.94	0.17	0.69	57.74	30.74	1.35	0.2	0.71	----	----	4.31

Table 4 Ash fusion characteristics of different carbonaceous substances in reducing conditions

Sample	Initial deformation temperature, K (IDT)	Softening temperature, K (ST)	Hemispherical temperature, K (HT)	Flow temperature, K (FT)
PC	1718	> 1773	> 1773	> 1773
SD	1450	1474	1483	1499
HAC	1661	> 1773	> 1773	> 1773

critical for the stable operation of an entrained flow gasifier [34]. On the other hand, it is necessary to operate fluidised bed and dry bottom fixed bed gasifiers below the AFT of the feed material to avoid ash agglomeration [35–38]. Ash composition and ash fusion temperature (AFT) of PC, SD and HAC have been shown in Tables 3 and 4, respectively. It is reflected that AFT of SD ash is lower than those of HAC and PC because of the higher concentrations of alkali and alkaline earth metal (AAEM) oxides (Na_2O , K_2O , CaO , MgO). These AAEM oxides are susceptible to form low-temperature eutectics resulting in the lowering of AFT. On the other hand, acidic oxides such as silica (SiO_2) and alumina (Al_2O_3) tend to increase AFT forming some high melting stable compounds of refractory nature during gasification [35]. Typical characteristics of Indian coal ash with higher concentrations of SiO_2 and Al_2O_3 lead to the higher AFT of HAC.

On the other hand, PC ash has a higher amount of vanadium oxide (V_2O_5) and nickel oxide (NiO), which makes it different from HAC and SD ash. In PC ash (wt%), generally, V_2O_5 , NiO , SiO_2 , Al_2O_3 , Fe_2O_3 and CaO together constitute around 95% and remaining 5% consists of MgO , TiO_2 , SO_3 , K_2O , Na_2O and P_2O_5 [28, 34, 39]. In general, petcoke ash has high AFT with IDT around 1450 °C and FT, even greater than 1500 °C due to the higher V_2O_5 . Wang et al. [40] also reported that the AFT of petcoke increases with increasing V_2O_5 concentration.

It is also established that the AAEM and iron act as catalysts in combustion and gasification reactions of carbonaceous substances. To examine the overall influence of catalytically active components, alkali index (AI) as proposed by Sakawa et al. [41] has been used for the present investigation and presented in Table 3. The influence of AI on char gasification behaviour has been discussed in sub-section “Effect of nature of char on gasification reactivity”.

3.3 CO_2 gasification reactivity and kinetics

3.3.1 Gasification reactivity of petcoke, sawdust and high ash coal char

In the present investigation, isothermal thermogravimetric gasification reactions of petcoke, sawdust and high ash coal char samples prepared at 1173 K were conducted at 1373, 1423,

1473, 1523 and 1573 K in CO_2 atmosphere. Carbon conversion (x) during gasification has been expressed as below:

$$x = (W_0 - W) / (W_0 - W_{\text{ash}}) \quad (1)$$

where W_0 , W and W_{ash} present the initial char weight, char weight at any time and ash weight in the char, respectively.

Plots of carbon conversion (x) versus reaction time (t) have been presented in Fig. 1. Gasification reactivity of different substances is generally compared by reactivity index, R , and it is defined as $R = 0.5/\tau_{0.5}$ (min^{-1}), where $\tau_{0.5}$ is the required time to achieve 50% carbon conversion [8, 9, 42]. This definition has been applied here to determine the gasification reactivity of PC char, HAC char and SD char. R values calculated from x versus t plots for different char samples have been shown in Fig. 2. The greater the reactivity index, R value of a particular char under definite condition, the higher is its reactivity.

Effect of temperature on gasification reactivity: Figures 1 and 2 clearly demonstrate that char gasification reaction becomes faster with the increasing temperature and gasification reactivity is noticeably influenced by gasification temperature irrespective of the nature of the char samples. As for example, reactivity index increases from 0.0081–0.0406 min^{-1} , 0.0746–0.1389 min^{-1} and 0.125–0.25 min^{-1} for PC char, HAC char and SD char, respectively in the temperature range of 1373–1573 K. This increase in reactivity index is owing to the endothermic nature of CO_2 -char gasification reaction. This trend is consistent with the findings of other researchers also [8, 9, 42]. Furthermore, it is worthy to mention here that gasification temperature not only influences the rate but also plays a crucial role to decide the rate-controlling step during reaction. For the present investigation, rate-controlling kinetics has been discussed in sub-section “Activation energy, Arrhenius plot and diffusion resistance”.

Effect of nature of char on gasification reactivity: Moreover, the order of gasification reactivity for different chars in the present investigation is SD char > HAC char > PC char throughout the studied conditions (Fig. 2). Much poorer gasification reactivity of PC char with respect to SD and HAC char can be explained from their physico-chemical properties. Pores are important in determining the reaction rate. Macro- and mesopores act as feeder pores for reaching the reactive gas to the active sites in the

Fig. 1 Conversion versus time relationships for char samples at a) 1373 K, b) 1473 K and c) 1573 K

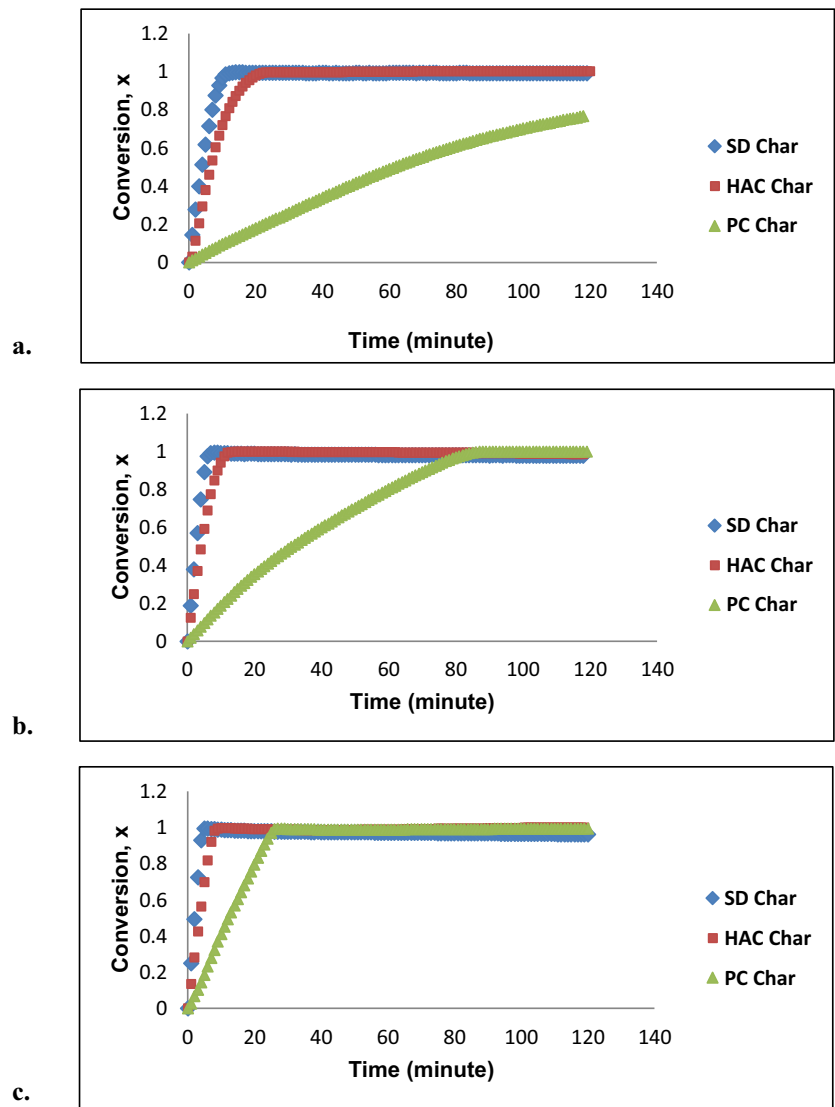


Fig. 2 Reactivity index (R , min^{-1}) of different char samples in the temperature range of 1373–1573 K

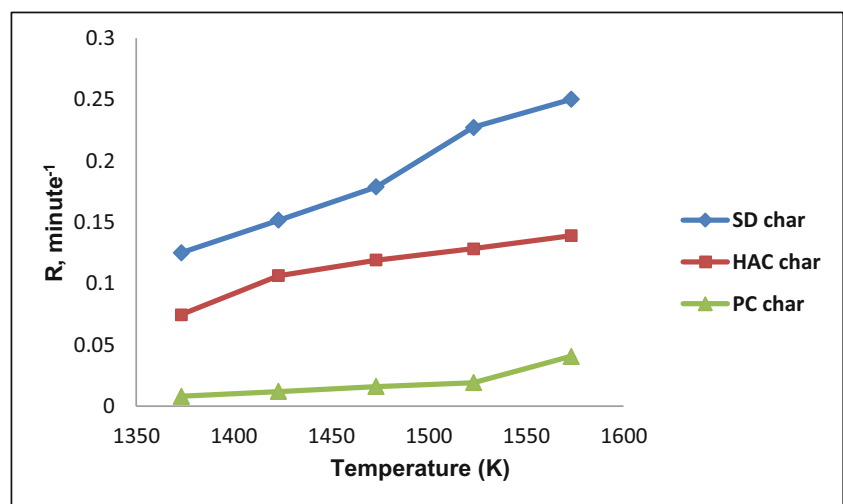


Table 5 Rate constant and activation energy of char samples at 1373–1573 K for homogeneous model (HM) and shrinking core model (SCM)

Sample	Gasification temperature (°C)	Rate constant (<i>k</i>) (homogeneous model, HM)	Activation energy (KJ/mol) (homogeneous model, HM)	Rate constant (<i>k</i>) (shrinking core model, SCM)	Activation energy (KJ/mol) (shrinking core model, SCM)
PC char	1100	0.0119	142.83	0.0033	142.59
	1150	0.0176		0.0049	
	1200	0.0242		0.0067	
	1250	0.0301		0.0084	
	1300	0.0674		0.0186	
SD char	1100	0.2066	56.24	0.0566	60.44
	1150	0.2726		0.0723	
	1200	0.3066		0.0856	
	1250	0.3592		0.1022	
	1300	0.3918		0.1099	
HAC char	1100	0.1227	59.93	0.0336	58.50
	1150	0.1652		0.0453	
	1200	0.2047		0.0547	
	1250	0.2230		0.0598	
	1300	0.2411		0.0655	

micropores, where the gasification reaction can occur. Therefore, proneness of gas-solid reaction is being enhanced with the

increasing char porous structure. In the present investigation, BET surface area (Table 2) sequence of different char samples

Fig. 3 Validation of **a)** homogeneous model (HM) and **b)** shrinking core model (SCM) for PC char at 1373–1573 K

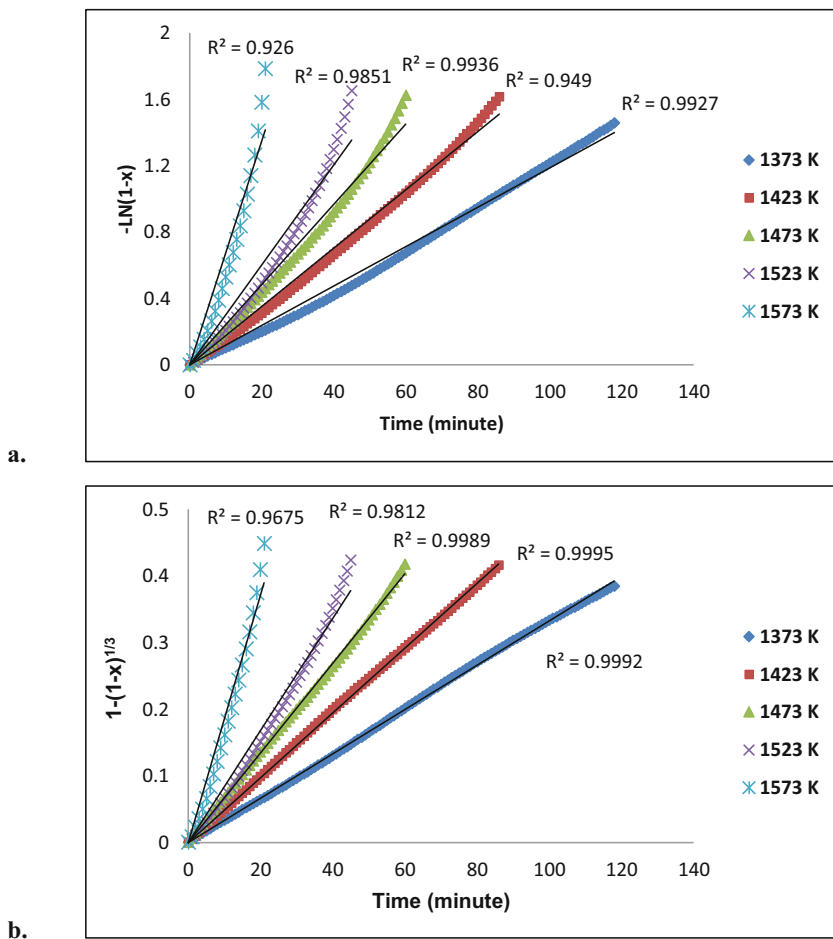
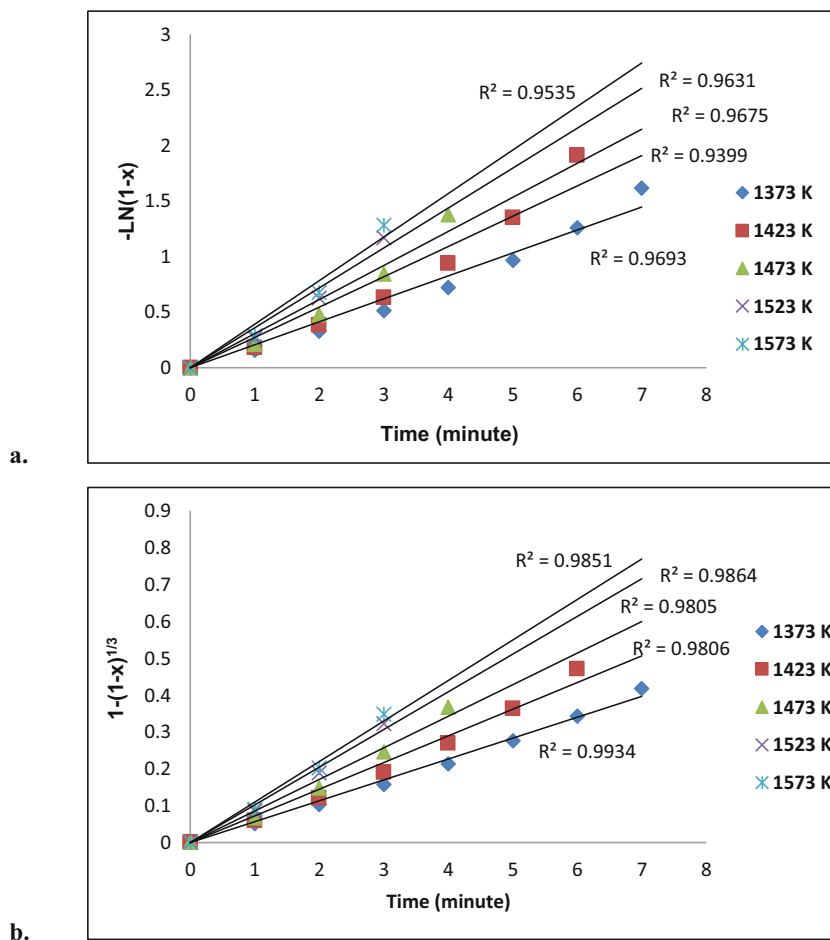


Fig. 4 Validation of **a)** homogeneous model (HM) and **b)** shrinking core model (SCM) for SD char at 1373–1573 K



is ranked as PC char < HAC char < SD char and char reactivity is found proportional to the BET surface area. This is in accordance with the findings obtained by other investigators [9, 43].

The catalytic activity of inorganic constituents of carbonaceous char is one of the factors found in literature to affect char gasification. Miura et al. [44] found that coal minerals control the gasification reaction of lower rank coal char ($C < 80\%$). Nature of char surface as well as the extent of oxygen functional groups is crucial for showing catalytic activity by inorganic constituents. Active metal (AAEM) cations must be present in exchangeable forms with carboxylic and phenolic groups to form active sites for performing catalytic activity. In the present study, sawdust, coal and petcoke differ significantly in their inorganic constituents, and sequence of AI which describes the overall influence of catalytically active species within the ash can be ranked as $SD > HAC > PC$ (Table 3) and AI has been found to be a good performer to explain the gasification reactivity. Additionally, carbon aromaticity, crystallinity and structural orderness differ significantly in PC, HAC and SD chars. PC char with the highest aromatic carbon, crystalline and compact structure shows very poor reactivity compared with HAC and SD char. Therefore, it may be summarised that AAEM concentrations (measured as AI) along with different

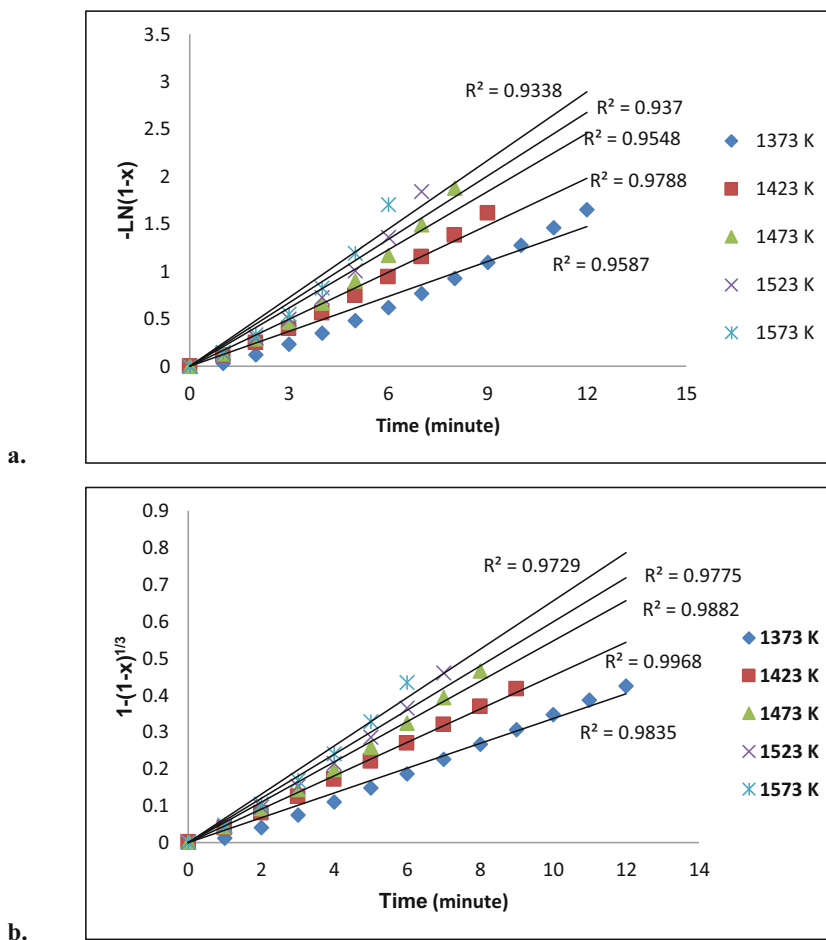
amounts of oxygen functional groups and porous structure (BET surface area) make the sequence of gasification reactivity as $SD \text{ char} > HAC \text{ char} > PC \text{ char}$.

3.3.2 Gasification kinetics of petcoke, sawdust and high ash coal char

Kinetic models: An extensive research has been conducted to develop kinetic models to explain various components of char gasification reaction. Though until now, there is no universal kinetic model for gasification reactions, various researchers have utilised different models. Among them, homogeneous model (HM), shrinking core model (SCM) and random pore model (RPM) are most widely applied. Considering the simplicity and efficiency to describe experimental data, homogeneous model (HM) and shrinking core model (SCM) have been utilised for CO_2 -char gasification kinetics in the present investigation [17, 42, 45, 46].

Homogeneous model (HM) simplifies the heterogeneous gas-solid reaction to a homogeneous reaction by assuming solid as a homogeneous assembly of small lumps of reactants. As per this model, a reaction occurs at all possible places, both the surface and the bulk. With the progress of the reaction, the

Fig. 5 Validation of **a)** homogeneous model (HM) and **b)** shrinking core model (SCM) for HAC char at 1373–1573 K



particle size remains the same, but density decreases. The rate equation for this model is expressed as

$$dx/dt = k_{HM} (1-x) \tag{2}$$

Its linearised solution is

$$-\ln (1-x) = k_{HM}t \tag{3}$$

where x is the conversion and k_{HM} is the rate constant. $-\ln (1-x)$ has been plotted against time, t , for all the char gasification reactions at 1373–1573 K under CO_2 atmosphere. The rate constant, k_{HM} , is obtained from the slope of the straight line and depicted in Table 5.

On the other hand, the shrinking core model (SCM) assumes that the reaction occurs at the surface of the solid or at the interface of the unreacted solid and the porous product layer. As per this model, the reaction takes place at the outer surface of a spherical particle. As the reaction proceeds, the reaction surface moves inward with the formation of an unreacted core which shrinks with time and leaves behind inert ashes. At the same time, it also assumes that the external radius of the particle remains the same assuming no deformation of the ash layer. It may be pointed out that, like HM, SCM

also does not consider structural changes of the solid during gasification reaction. The rate expression is

$$dx/dt = k_S (1-x)^{2/3} \tag{4}$$

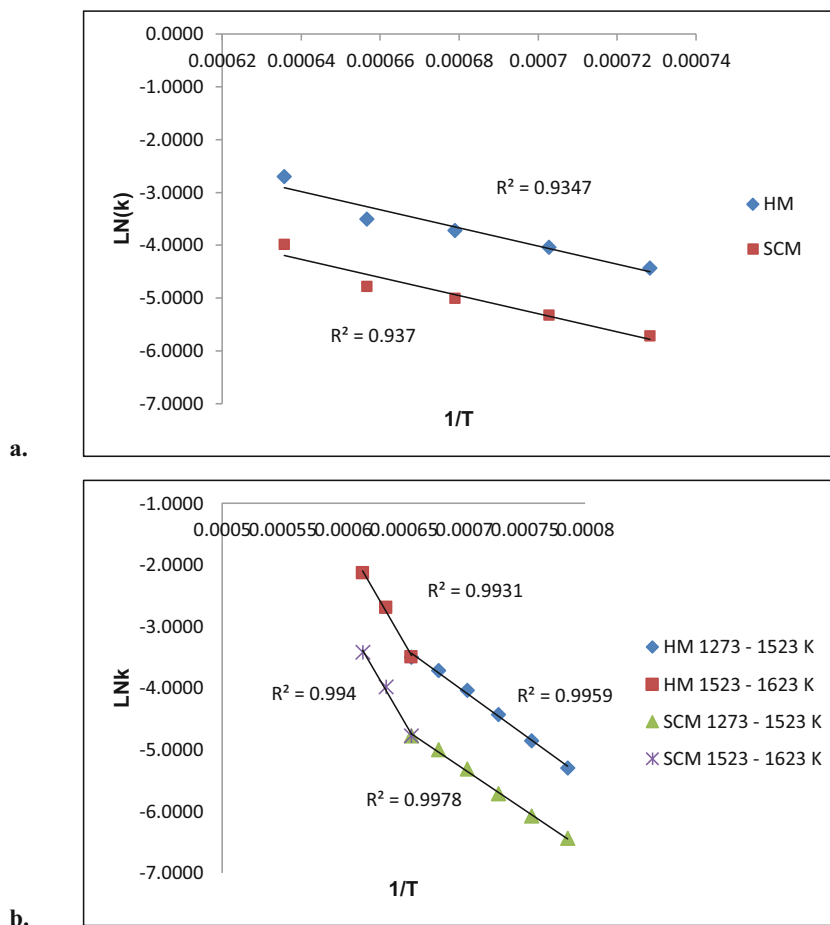
Its linearised solution is

$$1-(1-x)^{1/3} = k_S t \tag{5}$$

where x is the conversion and k_S is the rate constant. $1-(1-x)^{1/3}$ has been plotted against time, t , for all the experiments under studied conditions. The rate constant, k_S , has been obtained from the slope of the plot of $1-(1-x)^{1/3}$ versus t and depicted in Table 5.

Plots of $-\ln(1-x)$ versus t , and $1-(1-x)^{1/3}$ versus t for HM and SCM, respectively, have been presented in Figs. 3, 4 and 5 for PC char, SD char and HAC char in the temperature range of 1373–1573 K. These figures clearly illustrate that good linearities have been obtained for both the models. Values of correlation coefficients (R^2) of the straight lines have been shown in Figs. 3, 4 and 5. All the CO_2 char gasification experiments under the studied conditions have been well described by both HM and SCM. However, considering the correlation

Fig. 6 Arrhenius plots from homogeneous model (HM) and shrinking core model (SCM) for PC char in the temperature range of **a)** 1373–1573 K and **b)** 1273–1523 K and 1523–1623 K



coefficients (R^2) of both the models for all the PC, SD and HAC chars, it can be said that the overall fitting extent of SCM is better than that of HM. As for example, correlation coefficients (R^2) obtained from HM (Fig. 3a) for PC char vary from 0.926–0.9936, whereas R^2 values are found 0.9675–0.9995 for the same set of experiments in case of SCM (Fig. 3b). Similarly, R^2 obtained from HM and SCM for SD char are found to vary from 0.9399 to 0.9693 (Fig. 4a) and 0.9805–0.9934 (Fig. 4b), respectively. SCM is also found better to fit HAC char experiments with R^2 values of 0.9729–0.9968 (Fig. 5b) in comparison with the R^2 values of 0.9338–0.9788 (Fig. 5a) of HM. Therefore, SCM is found more suitable to describe CO_2 -char gasification reactions at 1373–1573 K for all the PC, SD and HAC chars in the present study. This finding matches with the observations reported in the literature [45, 46].

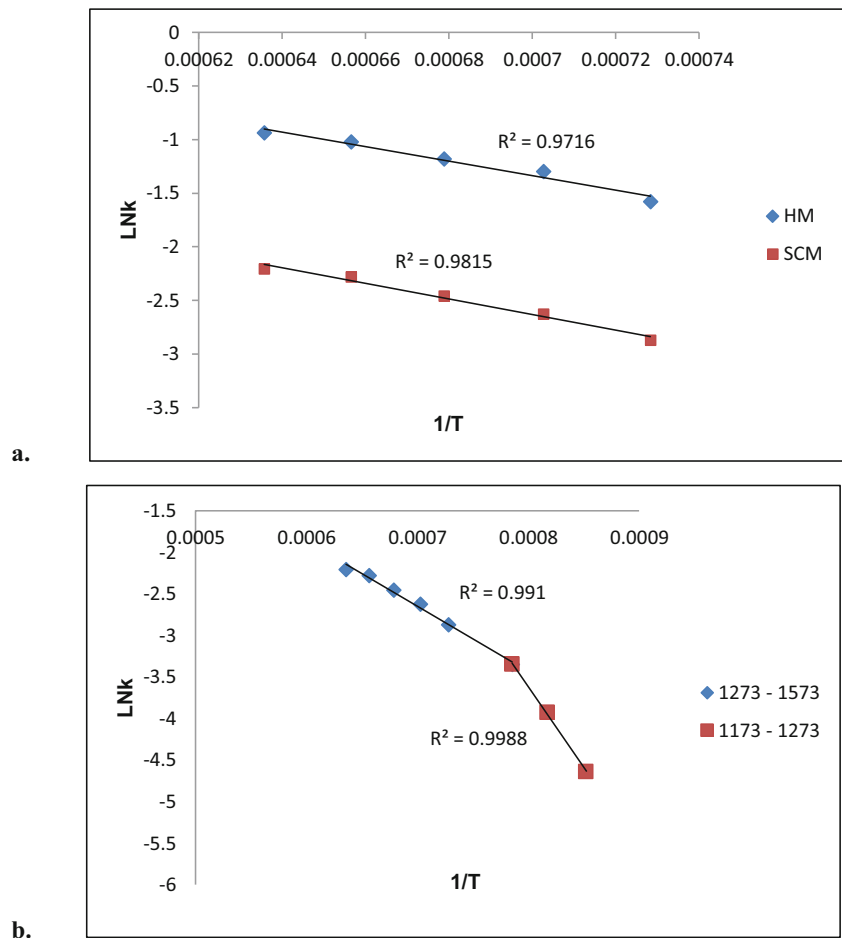
Moreover, values of rate constants, k_{HM} and k_{S} , are determined by HM and SCM, respectively, shown in Table 5, clearly demonstrate that (i) these rate constants increase with the increasing temperature under the studied conditions of 1373–1573 K and (ii) the sequence of rate constant values for different chars can also be ranked as SD char > HAC char > PC char.

Activation energy, Arrhenius plot and diffusion resistance: Activation energy, E (kJ/mol), for different char samples has been

determined from the slope of Arrhenius plot, $\text{Ln}k$ versus $1/T$, where k represents the corresponding rate constant of HM and SCM, and T is the absolute temperature. E values have been depicted in Table 5. Arrhenius plots for PC char, SD char and HAC char from HM and SCM in the temperature range of 1373–1573 K with correlation coefficients (R^2) are shown in Figs. 6a, 7a and 8a, respectively. As PC char is the least reactive among the three carbonaceous substances, E values for PC char are highest determined by both HM (142.83 kJ/mol) and SCM (142.59 kJ/mol) under the studied conditions. However, being the most active substance, E values of SD char are not always the lowest (Table 5). It may be due to the presence of diffusion resistance during gasification reactions under the studied conditions.

Saha [26] reported absence of diffusion resistance for CO_2 gasification kinetics of coal with particle sizes $-0.21 + 0.15$ mm in the temperature range of 1173–1323 K. As the present investigation is done with the same particle sizes but at higher temperature, there is a possibility of the presence of diffusion resistance. Therefore, to check the presence/absence of diffusion resistance, CO_2 gasification experiments with PC char of the same particle sizes were further conducted at 1273, 1323 and 1623 K, and kinetic analysis is done. Figure 6b shows the Arrhenius plots for PC char in the temperature range of 1273–1523 K and 1523–1623 K. Comparison of Fig. 6a with that of Fig. 6b clearly

Fig. 7 Arrhenius plots for SD char from **a**) homogeneous model (HM) and shrinking core model (SCM) at 1373–1573 K and **b**) shrinking core model at 1173–1273 K and 1273–1573 K



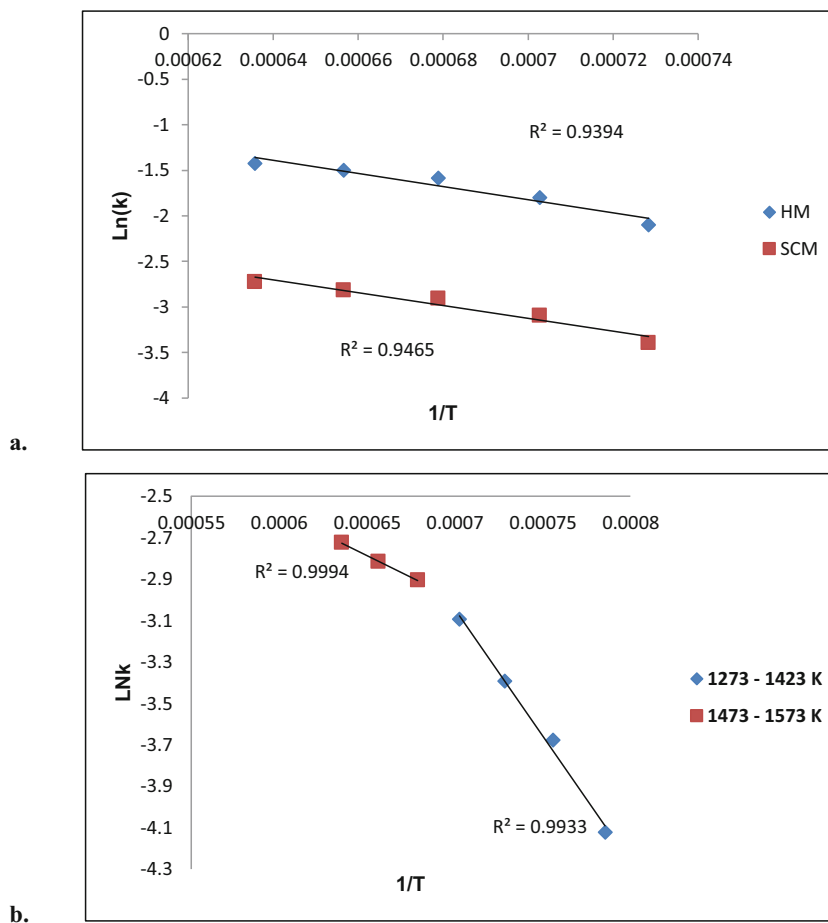
exhibits that there is a clear deviation in linearity in Arrhenius plots for PC char from HM and SCM at 1523 K. R^2 of Arrhenius plots from HM and SCM at 1373–1573 K are 0.9347 and 0.937, respectively (Fig. 6a), whereas Arrhenius plots for PC char at 1273–1523 K and 1523–1623 K show high linearity with R^2 of 0.9959 and 0.9931 for HM, and 0.9978 and 0.994 for SCM, respectively (Fig. 6b). It is therefore justified to infer that diffusion resistance starts for PC char gasification reactions in CO_2 atmosphere with particle sizes $-0.21 + 0.15$ mm above 1523 K and CO_2 -char gasification of PC char in the temperature range of 1273–1523 K is pure chemically controlled.

Figure 7a shows Arrhenius plots for SD char from HM and SCM at 1373–1573 K with R^2 of 0.9716 and 0.9815, respectively. As the linearity is quite good, there may be a possibility of beginning diffusion resistance below 1373 K. Therefore, to test the presence of diffusion factor for SD char, CO_2 gasification reactions with the same particle sizes were further performed at 1173–1273 K. Arrhenius plots for SD char from SCM at 1173–1273 K (R^2 is 0.9988) and 1273–1573 K (R^2 is 0.991) in Fig. 7b unequivocally demonstrate that diffusion resistance starts for SD char gasification reaction with particle sizes $-0.21 + 0.15$ mm in CO_2 above 1273 K and SD char gasification kinetics up to 1273 is definitely pure chemically controlled.

Similarly, to check the presence/absence of diffusion resistance in CO_2 gasification for HAC char in the temperature range of 1373–1573 K, gasification experiments with the same particle sizes were carried out at 1273 and 1323 K. Figure 8b shows the Arrhenius plots for HAC char from SCM at 1273–1423 K and 1473–1573 K with R^2 of 0.9933 and 0.9994, respectively. This figure evidently demonstrates that diffusion resistance is present above 1423 K for HAC char and CO_2 gasification kinetics up to 1423 K with particle sizes $-0.21 + 0.15$ mm is chemically controlled.

Therefore, it may be said that diffusion resistance is present in CO_2 gasification for PC char and HAC char with particle sizes $-0.21 + 0.15$ mm in the temperature range of 1373–1573 K, whereas the said resistance is visible for SD char with the same particle sizes at 1273–1573 K. Diffusion resistance in CO_2 gasification kinetics starts for PC char, SD char and HAC char above 1523 K, above 1273 K and above 1423 K, respectively. This difference in gasification behaviour for different chars is attributed to their differences in AFT. Char structure becomes less permeable to the reactive gas with the softening of mass at high-temperature gasification. Lower AFT causes softening of the mass at a lower temperature range to happen. It is therefore justified to mention that diffusion

Fig. 8 Arrhenius plots for HAC char from **a**) homogeneous model (HM) and shrinking core model (SCM) at 1373–1573 K and **b**) shrinking core model at 1273–1423 K and 1473–1573 K



resistance comes in force at lower gasification temperature with the lowering of AFT range of the ash. Consequently, SD char kinetics is being affected first by diffusion resistance with its lowest AFT followed by HAC char with its medium AFT and finally PC char kinetics shows diffusion resistance at the highest temperature with its highest AFT under this study. Gu et al. [17] reported similar observation for CO₂ gasification kinetics of petcoke and low ash coal. However, reporting of diffusion resistance in CO₂ gasification kinetics for high ash coal, biomass and petcoke is very rare in literature.

4 Conclusion

The present paper compares CO₂-char gasification reactivity and kinetics of petcoke, sawdust and high ash coal with their physico-chemical properties under isothermal conditions in the temperature range of 1173–1623 K. Based on the results obtained and subsequent discussion, it is reasonable to infer as below:

i) The higher amount of cross-links and oxygen functional groups in sawdust and coal lead to the larger volatiles which on removal during heating produce more porous chars. On the other hand, the structural makeup of

petcoke with less volatile matter and less oxygen functional groups makes it less porous.

- ii) AFT of sawdust ash is lower than those of coal and petcoke because of the higher concentrations of AAEM oxides. The refractory nature of Indian coal ash with higher concentrations of SiO₂ and Al₂O₃ leads to its higher AFT. On the other hand, a large amount of V₂O₅ and NiO makes petcoke ash different from coal and biomass ash. AFT of petcoke ash is found highest in this study.
- iii) AAEM concentrations (measured as AI) along with different amounts of oxygen functional groups and porous structure (BET surface area) make the sequence of gasification reactivity in the present investigation as SD char > HAC char > PC char.
- iv) Homogeneous model (HM) and shrinking core model (SCM) have been utilised for CO₂-char gasification kinetics in the present investigation. Considering the correlation coefficients (R^2) of both the models for all the PC, SD and HAC chars, it can be said that SCM is found more suitable to describe CO₂-char gasification reactions in the temperature range of 1373–1573 K.
- v) Activation energy of PC char is found higher than that of HAC and SD char. However, activation energy of

SD char, though it is the most active substance, is not always the lowest.

- vi) Diffusion resistance is found to exist in CO₂ gasification kinetics for PC char and HAC char with the particle sizes $-0.21 + 0.15$ mm in the temperature range of 1373–1573 K, whereas the said resistance is present for SD char with the same particle sizes at 1273–1573 K. Diffusion resistance starts for PC char, SD char and HAC char above 1523 K, above 1273 K and above 1423 K, respectively.

Acknowledgements The authors are thankful to the Director, CSIR-Central Institute of Mining and Fuel Research, Dhanbad, for allowing the publication of this paper.

Funding information The authors received financial support from the CSIR (Ministry of Science and Technology, Govt. of India), New Delhi, through the FBR Project (MLP-75/18-19) under Chemical Theme.

References

- Annual Report 2018–19, Energizing and empowering India, Ministry of Petroleum and Natural Gas, Govt. of India
- Nemanova V, Abedini A, Liliedahl T, Engvall K (2014) Co-gasification of petroleum coke and biomass. *Fuel* 117:870–875
- Item No. 2, Court No. 4, Section PIL-W, Record of Proceedings, Supreme Court of India, Writ Petition (Civil) No. 13029/1985, 24.10.2017
- Item No. 16, Court No. 3, Section PIL-W, Record of Proceedings, Supreme Court of India, Writ Petition (Civil) No. 13029/1985, 26.07.2018
- Report on Indian Coal and lignite Resources (2018) Under natural energy resources, mission –II B, 2018. Geological Survey of India, Govt. of India
- Website of Ministry of New and Renewable Energy, Govt. of India, www.mnre.gov.in/bio-energy/current-status
- Wang G, Zhang J, Huang X, Liang X, Ning X, Li R (2018) Co-gasification of petroleum coke-biomass blended char with steam at temperatures of 1173–1373 K. *Appl Therm Eng* 137:678–688
- Saha S, Sahu G, Chavan PD, Datta S (2018) Gasification reactivity of high ash Indian coals in varying concentrations of CO₂. *Int. Journal of Oil, Gas and Coal Technology* 18:163–186
- Huo W, Zhou Z, Chen X, Dai Z, Yu G (2014) Study on CO₂ gasification reactivity and physical characteristics of biomass, petroleum coke and coal chars. *Bioresour Technol* 159:143–149
- Fermoso J, Gil MV, Borrego AG, Pevida C, Pis JJ, Rubiera F (2010) Effect of the pressure and temperature of devolatilization on the morphology and steam gasification reactivity of coal chars. *Energy and Fuels* 24:5586–5595
- Hattingh BB, Everson RC, Neomagus HWJP, Bunt JR (2011) Assessing the catalytic effect of coal ash constituents on the CO₂ gasification rate of high ash, South African coal. *Fuel Process Technol* 92:2048–2054
- Liu T, Fang Y, Wang Y (2008) An experimental investigation into the gasification reactivity of chars prepared at high temperatures. *Fuel* 87:460–466
- Saha S, Sharma BK, Chavan PD, Datta S, Sahu G, Mall BK, Sharma T (2011) Effect of inorganic matter on the reactivity of Indian coals. *Asian J Chem* 23:4335–4340
- Ding L, Wei J, Dai Z, Guo Q, Yu G (2016) Study on rapid pyrolysis and in-situ char gasification characteristics of coal and petroleum coke. *International Journal of Hydrogen Energy* 41:16823–16834
- Ding L, Zhou Z, Huo W, Yu G (2015) Comparison of steam-gasification characteristics of coal char and petroleum coke char in drop tube furnace. *Chin J Chem Eng* 23:1214–1224
- Zhan X, Jia J, Zhou Z, Wang F (2011) Influence of blending methods on the co-gasification reactivity of petroleum coke and lignite. *Energy Convers Manag* 52:1810–1814
- Gu J, Wu S, Zhang X, Wu Y, Gao J (2009) CO₂-gasification reactivity of different carbonaceous materials at elevated temperatures. *Energy Sources, Part A: Recovery, Utilization, and Environmental Effects* 31:232–243
- Fermoso J, Arias B, Pevida C, Plaza MG, Rubiera F, Pis JJ (2008) Kinetic models comparison for steam gasification of different nature fuel chars. *J Therm Anal Calorim* 91:779–786
- Ren L, Yang J, Gao F, Yan J (2013) Laboratory study on gasification reactivity of coals and Petcoke in CO₂/steam at high temperatures. *Energy Fuel* 27:5054–5068
- Wu Y, Wu S, Gu J, Gao J (2009) Differences in physical properties and CO₂ gasification reactivity between coal char and petroleum coke. *Process Saf Environ Prot* 87:323–330
- Afroz IE, Ching DLC (2019) A modified model for kinetic analysis of petroleum coke. <https://doi.org/10.1155/2019/2034983>
- Datta S, Chauhan V, Sahu G, Chavan PD, Saha S, Gupta PK, Dutta P (2019) Co-gasification of high ash Indian coal-biomass blends in a pilot-scale fluidized bed gasifier. *Biomass Conversion and Biorefinery*. <https://doi.org/10.1007/s13399-019-00567-2>
- Saha S, Sharma BK, Kumar S, Sahu G, Badhe YP, Tambe SS, Kulkarni BD (2007) Density measurements of coal samples by different probe gases and their interrelation. *Fuel* 86:1594–1600
- Chavan P, Datta S, Saha S, Sahu G, Sharma T (2012) Influence of high ash Indian coals in fluidized bed gasification under different operating conditions. *Solid Fuel Chemistry* 46:108–113
- Kristiansen A (1996) Understanding of coal gasification, IEA coal research report IEACR/86. International Energy Agency, London
- Saha S (2013) Studies on physical properties of Indian coals and its effect on coal gasification kinetics. Ph.D. Thesis, Indian School of Mines (ISM), Dhanbad, India
- Saha S, Sahu G, Datta S, Chavan PD, Sinha AK, Sharma BK, Sharma T (2013) Studies on CO₂ gasification reactivity of high ash Indian coal. *International Journal of Emerging Technology and Adv Engineering* 3:29–33
- Li J, Chen X, Liu Y, Xiong Q, Zhao J, Fang Y (2017) Effect of ash composition (Ca, Fe and Ni) on petroleum coke ash fusibility. *Energy Fuel* 31:6917–6927
- Patil-Shinde V, Saha S, Sharma BK, Tambe SS, Kulkarni BD (2016) High ash char gasification in thermo-gravimetric analyzer and prediction of gasification performance parameters using computational intelligence formalisms. *Chem Eng Commun* 203:1029–1044
- In: Karr CJ (Ed) Analytical methods for coal and coal product (1978). Volume 1, Academic press, London, 1978
- Zuo HB, Zhang PC, Zhang JL, Bi XT, Geng WW, Wang GW (2015) Gasification and kinetic models. *BioResources* 10:5242–5255
- Lewis AD, Fletcher EG, Thomas H, Fletcher TH (2014) CO₂ gasification rates of petroleum coke in a pressurized flat-flame burner entrained-flow reactor. *Energy Fuels* 28:4447–4457
- Naredi P, Pisupati SV (2008) Interpretation of char reactivity profiles obtained using a thermogravimetric analyzer. *Energy Fuel* 22:317–320
- Li J, Xiong Q, Shan J, Zhao J, Fang Y (2018) Investigating a high vanadium petroleum coke ash fusibility and its modification. *Fuel* 211:767–774

35. Datta S, Sarkar P, Chavan PD, Saha S, Sahu G, Sinha AK, Saxena VK (2015) Agglomeration behaviour of high ash Indian coals in fluidized bed gasification pilot plant. *Appl Therm Eng* 86:222–228
36. Kamble AD, Saxena VK, Chavan PD, Mendhe VA (2019) Co-gasification of coal and biomass an emerging clean energy technology: status and prospects of development in Indian context. *Int J Min Sci Technol* 29:171–186
37. Datta S, Chavan PD, Sahu G, Saha S, Dutta P, Sarkar P, Saxena VK (2018) Gasification of coal and press mud blends in fluidized bed gasifier. *Int. Journal of Oil, Gas and Coal Technology* 19:248–262
38. Chavan PD, Sharma T, Mall BK, Rajurkar BD, Tambe SS, Sharma BK, Kulkarni BD (2012) Development of data-driven models for fluidized-bed coal gasification process. *Fuel* 93:44–51
39. Xiong Q, Li J, Guo S, Li G, Zhao J, Fang Y (2018) Ash fusion characteristics during co-gasification of biomass and petroleum coke. *Bioresour Technol* 257:1–6
40. Wang ZG, Bai J, Kong LX, Bai ZQ, Li W (2013) Effect of V and Ni on ash fusion temperatures. *Energy Fuel* 27:7303–7313
41. Sakawa M, Sakurai Y, Hara (1982) Influence of coal characteristics on CO₂ gasification. *Fuel* 61:717–720
42. Zhang L, Huang J, Fang Y, Wang Y (2006) Gasification reactivity and kinetics of typical Chinese anthracite chars with steam and CO₂. *Energy Fuel* 20:1201–1210
43. Zhu WK, Song WL, Lin WG (2008) Catalytic gasification of char from co-pyrolysis of coal and biomass. *Fuel Process Technol* 89: 890–896
44. Miura K, Hashimoto K, Silveston PL (1989) Factors affecting the reactivity of coal chars during gasification, and indices representing reactivity. *Fuel* 68:1461–1465
45. Kwon TW, Kim SD, Fung DPC (1988) Reaction kinetics of char – CO₂ gasification. *Fuel* 67:530–535
46. Kim YT, Seo DK, Hwang J (2011) Study of the effect of coal type and particle size on char-CO₂ gasification via gas analysis. *Energy Fuel* 25:5044–5054

Publisher's note Springer Nature remains neutral with regard to jurisdictional claims in published maps and institutional affiliations.